Translational Oncology
www.transonc.com

Volume 12 Number 8 August 2019 pp. 1113–1121 1113

Ultrasonic Cavitation Ameliorates Antitumor Efficacy of Residual Cancer After Incomplete Radiofrequency Ablation in Rabbit VX2 Liver Tumor Model[1]

Shi-yan Li[*], Pin-tong Huang[†], Yong Fang[‡], Yao Wu[*], Ling Zhou[*], Jie-li Luo[†], Xian-chen Wang[*] and Yun-chong Chen[*]

[*]Department of Ultrasound, Sir Run Run Shaw Hospital, Zhejiang University, School of Medicine, Hangzhou, Zhejiang Province, China; [†]Department of Ultrasound, The Second Affiliated Hospital of Zhejiang University, School of Medicine, Hangzhou, Zhejiang Province, China; [‡]Department of Oncology, Sir Run Run Shaw Hospital, Zhejiang University, School of Medicine, Hangzhou, Zhejiang Province, China

Abstract

Residual cancer after incomplete ablation remains a major problem for radiofrequency ablation (RFA). We aimed to investigate the synergetic treatment efficacy of RFA combined with ultrasonic cavitation for liver tumor. Sixty rabbits with VX2 liver tumor were randomly divided into three groups. Group A was control group without any treatment. Combined ultrasonic cavitation with RFA was performed for group B1. Group B2 underwent RFA alone. The histopathological results were compared at the 5th, 11th, and 18th day of experiment, and the survival time and metastasis were assessed. The tumor volume growth rate, percentage of necrosis area, microvessel density, and apoptosis index showed significant differences among these groups at the 5th day, 11th day, and 18th day of experiment ($P < .05$). In contrast, the difference of metastatic score was not significant at the 5th and 11th day ($P > .05$). At the 18th day, the metastatic score of group A was significant higher than that of group B1 ($P < .05$), whereas the differences between group A and group B2, or group B1 and group B2 were not significant ($P > .05$). The median/range interquartile of survival time in groups A, B1, and B2 were 25/8 days, 50/19 days, and 48/20 days, respectively, and there was significant difference between groups A and B1 or B2 ($P < .05$). The difference between groups B1 and B2 was not significant ($P > .05$). Ultrasonic cavitation after incomplete RFA for liver tumor improved the antitumor effect, which could be considered as a potentially useful combined therapeutic strategy for liver malignancy.

Translational Oncology (2019) 12, 1113–1121

Introduction

Liver cancer is predicted to be the sixth most commonly diagnosed cancer and the fourth leading cause of cancer death worldwide in 2018 [1]. Of these, China have accounted for 50% of the total number of cases and deaths [2]. In addition to surgical resection, liver transplantation provides an alternative therapy for unresectable liver tumors. However, these treatments are limited for some reasons, including severe liver dysfunction and shortage of liver grafts [3–5]. Thus, several minimally invasive local treatments have been applied for liver cancer, of which radiofrequency ablation (RFA) is widely used [6]. RFA is considered as the best option for inoperable hepatocellular carcinoma (HCC) in patients, who have no more than three liver nodules, a maximum 3 cm diameter tumor, and preserved

Address all correspondence to: Pin-tong Huang, MD, Department of Ultrasound, The Second Affiliated Hospital of Zhejiang University, School of Medicine, No. 88, Jiefang Road, Hangzhou 310009, Zhejiang Province, China.
E-mail: huangpintong@zju.edu.cn
[1] Declarations of interest: none.
Received 1 March 2019; Accepted 8 May 2019

1936-5233/19
https://doi.org/10.1016/j.tranon.2019.05.007

liver function (Child-Pugh A and B) [7,8]. Although image-guided RFA is effective, simple, safe, and repeatable, residual cancer after incomplete ablation remains a major problem for RFA that troubles the clinical practice for several years. Previous studies reported that the local recurrent rates of RFA ranged from 49% to 74% [9–11]. Besides, invasiveness of residual cancer has been demonstrated after RFA as compared with patients without RFA [12,13].

Cavitation is the response of gas bubbles in liquid after oscillating to an acoustic field [14–16], which is one of major physical effects of ultrasound. Under certain ultrasound excitation, microbubble in liquid is irritated as vigorous contraction, expansion, oscillation, and even implosion, resulting in extreme local physical phenomenon, such as high pressure, shock wave, and microjets. In the presence of large amount of exogenous cavitation nuclei, for example, lipid microbubbles injected into circulation, inertial cavitation might be induced, which can cause sonoporation or capillary destruction. This process can result in hemorrhage, edema, thrombus formation, and damage to the endothelium of capillaries or small vessels in various tissues [17–19], which can induce necrosis and apoptosis of cancer cells and inhibit tumor growth [20,21]. It has been reported that ultrasonic cavitation is an effective application for tumor vasculature destruction or antitumor effects [22–26].

Recurrence after RFA is a major drawback in the management of HCC, and effective adjuvant therapies are urgently needed [27]. Combined treatment, for example, chemotherapy or radiation with hyperthermia, may be an effective strategy for cancer. Bholee et al. [28] compared the effectiveness of transarterial chemoembolization (TACE) combined with RFA versus hepatectomy for HCC within Milan criteria, and the results showed that TACE+RFA is safe and as effective as hepatectomy for patients. In another study, the efficacy of sorafenib combined with RFA for treating HCC was investigated, and the findings demonstrated that the RFA efficiency has been enhanced with sorafenib [29]. For the ultrasonic cavitation, Zhao et al. [30] reported that the degree of coagulation during pulsed high-intensity focused ultrasound could be enhanced by cavitation. Additionally, ultrasound-triggered microbubble destruction is an effective adjunct when combined with radiotherapy to treat HCC compared with radiotherapy alone [31]. Then, as far as RFA in combination with ultrasonic cavitation was concerned, whether antitumor efficacy could be improved is worth to be further investigated. To date, the report of this novel combined strategy is rare. Therefore, the present study aimed to assess the synergetic treatment efficacy of RFA combined with ultrasonic cavitation for incomplete ablated liver tumor in a rabbit model.

Materials and Methods

This study was approved by the laboratory animal ethics committee of our institution and abided by the criteria outlined by the National Institutes of Health Guide for the Care and Use of Laboratory Animals.

VX2 Liver Tumor Model and Experimental Groups

The liver tumors was induced by referring to the method of Haaga et al. [32]. VX2 tumor was propagated in male New Zealand white rabbits that were selected randomly from the experimental animal center of out university.VX2 carcinoma cells (Hangzhou Hibio Technology Co., Ltd., Hangzhou, China) were injected intramuscularly into the hind legs of the sedated rabbits. When the tumor diameter reached 2 cm, the tumor was harvested from the anesthetized animals by using sterile techniques. The fresh hoary fish meat-like tumor tissues were obtained and stored in liquid nitrogen. The necrotic tissue, the surrounding connective tissue, and the fat were removed. When it will be transplanted into the liver, the tumor tissues were thawed rapidly at 36°C.

Sixty male New Zealand white rabbits (weighing 2.5-3.4 kg, average 2.96 ± 0.24 kg) were anesthetized by injection with 3% pentobarbital solution into auricular vein at a dosage of 30 mg/kg body weight or different dose based on different animal status in order to make sure that the breath of animals was slowest, other than for the dead ones, and stable, which was assessed when half of the scheduled dose was performed and how many remaining dose should be used was decided according to this assessment.

The thawed harvested tumor tissue was dissected into cubes of 2 mm^3. The abdomen of the experimental animals was shaved and cleared with povidone iodine solution before tumor implantation, then a small midline incision was made at the subxiphoid process, and the left medial lobe of the liver was exposed and exteriorized. The capsule of the liver was punctured with ophthalmic forceps, and the prepared small piece of VX2 tumor was inserted into the liver parenchyma at a depth of 0.5-1 cm. Hemostasis was achieved by applying gelatin sponge and manual pressure to the liver surface for 2-3 minutes. The abdominal muscles and skin were closed with an absorbable suture. The transplanted rabbits were injected with 50,000 IU/kg of penicillin sodium once a day for 3 consecutive days after inoculation.

When the transplanted VX2 tumor diameter reached anticipated size (about 1.5-2.0 cm) detected by ultrasonography in about 3-5 weeks, they were used for our experiments. All of these 60 transplanted rabbits were randomly divided into two groups firstly: group A was control group (20 animals) without any treatment; group B was therapeutic group (40 animals), animals which underwent incomplete RFA for establishing residual tumor model and were further divided into two subgroups randomly. The combined therapy with ultrasonic cavitation following RFA was performed for group B1 (20 animals), and RFA followed by pretending to irradiate with saline replaced microbubbles was performed for group B2 (20 animals).

Model of Residual VX2 Liver Tumor Following RFA

The same anesthesia protocol as for carcinoma implantation was used during RFA procedure. A grounding pad was applied for the animal's shaved flank before RFA. The abdomen of the experimental rabbits was shaved and prepared with povidone iodine, and percutaneous ultrasound-guided RFA was performed by using Philips IU22 ultrasound system (Philips Ultrasound Inc., Reedsville, PA) with an L9-3 probe (frequency 3-9 MHz). A radiofrequency generator (VIVA; STARmed, Goyang, Korea) along with an 18-gauge monopolar internally cooled electrode (VIVA; STARmed) was used to generate RF energy. The radiofrequency electrode had a 7-cm length shaft with a 0.7-cm active tip and cooled by a water circulation pump (VIVA pump; STARmed). Each ablation cycle lasted for 3 minutes with 30 W of power output, which could induce approximate 1.1 × 1.0 cm of coagulative necrosis region according to the manufacturer's recommendations. The tumor center was also designated as the center of ablated zone. Since the ablation region was smaller than the lesion, residual tumor was left surrounding to the ablation region (Figure 1*A*).

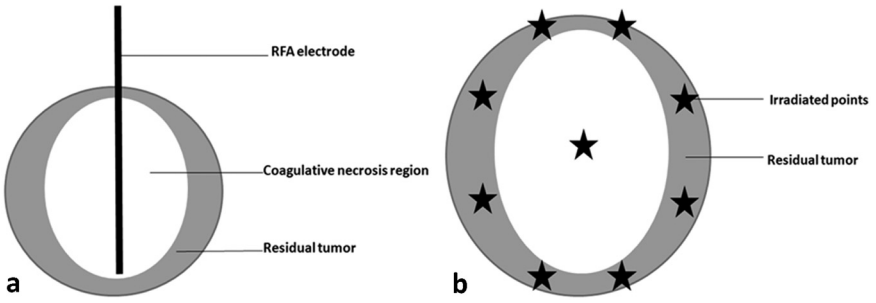

Figure 1. Schematic diagram of arrangement of RFA electrode for inducing residual tumor (A) and irradiated points for ultrasonic cavitation (B).

Microbubble Preparation, Contrast-Enhanced Ultrasonography, and Acoustic Cavitation Treatment

The microbubble contrast agent SonoVue (Bracco SpA, Milan, Italy) was supplied as a lyophilized powder; it was reconstituted by adding 5 ml of saline and gently shaking the vial by hand to form a homogeneous microbubble suspension, which contains about 2×10^8 sulfur hexafluoride-filled microbubbles (2.5 μm in average diameter) per milliliter, according to the manufacturer's recommendations [33]. Prior to each injection, microbubbles were resuspended by shaking the vial. The agent was administered as a bolus injection through a 20-gauge catheter. The dosage of contrast medium was 0.02 ml/kg body weight for both imaging and cavitation procedure.

The day on which the RFA procedure was performed for group B was defined as the first day of experiment. Contrast-enhanced ultrasound (CEUS) imaging of the rabbit liver was performed five times for the group B (before RFA, after RFA immediately, the 5th day, 11th day, and 18th day of experiment) and four times for the group A (before experiment, the 5th day, 11th day, and 18th day of experiment). We used an L9-3 liner array transducer (IU22, Philips) with a low mechanical index (0.07) of the pulse inversion harmonic imaging mode. The ultrasound probe was placed on the subxyphoid region. Grayscale ultrasound was used to determine the location and echogenicity of the lesions. The SonoVue was injected as a bolus into the auricular vein followed by 2-ml saline flush. CEUS images were stored digitally. The maximum length, width, and thickness of the tumors and the ablation regions were determined from the two vertical largest slices on CEUS images and were measured by two sonologists independently. The volume of tumor and ablation zone was calculated using the following formula [34]. The mean volume of the two sonologists was used for evaluating the treatment response.

$$\text{Volume} = 1/2(\text{length} \times \text{width} \times \text{thickness})$$

The animals in group B1 received ultrasonic cavitation treatments daily over three consecutive days after the RFA treatment (the second, third, and fourth day of experiment). The anesthesia protocol was same as the RFA procedure. After coupled using acoustic coupling gel, the transducer from a sonicator equipped with a 1-cm^2 transducer cone tip (Haiying Medical Electronic Instrument Company, Wuxi, China) was used to irradiate the tumor. Ultrasonic cavitation was performed at a frequency of 370 kHz, output voltage of 440 mV, and acoustic pressure of 1.55 MPa. Nine irradiated points around the lesion were arranged before cavitation (Figure 1*B*) by a careful localization using a linear array probe (LA332) of ultrasound imaging system (MyLab 90, Esaote, Italy) which was fixed and had the same focus position with the irradiated transducer. There were 15 therapy cycles for each irradiated point which were composed by 9-second pause followed by 1-second irradiation (10% duty cycle). Microbubbles were administrated three times during the cavitation therapy for each irradiated point: the first zero second, the 50th second, and the 100th second, respectively; and the dosage of each injection was the same as the CEUS examination.

Evaluation of Antitumor Effects

At the 5th day, the 11th day, and the 18th day of experiment, respectively, five animals in group A, group B1, and group B2 were selected randomly and sacrificed by intravenous anesthesia overdose, before which CEUS was performed. The tumor tissue was surgically excised for histological examination. The tumor volume was measured by drainage before fixed. The tumor volume growth rate (TVGR) at *n* day was calculated based on the following equation:

$$[(Vn - V\text{initial})/V\text{initial}] \times 100\%$$

Vn and *V*initial were the tumor volume of each group measured at *n* day after treatment and start of treatment, respectively.

The thoracic and abdominal exploration was performed to detect the metastatic lesions. A score method was used to assess the metastasis. Intrahepatic metastasis, abdominal metastasis, and thoracic metastasis were scored 1 point, respectively, and all the points were added as the total score. If no metastasis was found, 0 point was recorded.

The harvested tumor tissues were fixed in formalin and embedded in paraffin. Then samples were cut into 4-mm cryosections and stained with hematoxylin and eosin (H&E) using a standard protocol for gross histologic assessment of cellular density, necrosis, and fibrosis. Images of tumor sections stained with H&E were acquired, and the percentage of necrotic area was assessed with a stereomicroscope (Olympus BX43, Olympus Co, Tokyo, Japan) using a ×40 and ×100 objective.

The degree of apoptosis was evaluated with terminal deoxynucleotidyl transferase-mediated dUTP nick-end labeling (TUNEL). The cell nucleus was stained with 4,6-diamidino-2-phenylindole (DAPI). Three views using a ×200 objective were selected randomly to calculate the number of cells that stained positive for TUNEL, and the average number of these three views was defined as the apoptosis index.

Angiogenesis of tumor was assessed by calculating the microvessel density (MVD). Immunohistochemical staining was performed on the specimens with anti-CD34 monoclonal antibody (BOSTER

Biological Technology Co., Ltd., Wuhan, Hubei Province, China) according to the avidin-biotin peroxidase complex technique for evaluation. CD34-positive cells and cell clusters relative to adjacent areas were classified as "hot spots" in areas of higher density [35]. The pathology sections were initially screened at low power (×40) to identify areas with the largest numbers of microvessels or vascular hot spots. Then, the microvessels were counted in three high-power fields (×200). The MVD was calculated as the mean number of microvessels in these three most vascularized areas [36].

The remaining five rabbits in group A, group B1, and group B2 were raised and checked twice every day for observing the survival. The humane end point was defined by >50% decrease in food intake and >20% loss in body weight. Then they were humanely euthanized by injection of overdose 3% pentobarbital solution (>3 ml/kg) via ear vein.

Statistical Analysis

SPSS software (version 19.0, SPSS Inc., Chicago, IL) was used to perform the statistical analysis. Continuous data were expressed as mean ± standard deviation. Comparisons among different groups were performed using one-way analysis of variance and least significant difference, or Student's *t* test. Ranked data were expressed as median and range interquartile, and Kruskal-Wallis *H* test was carried out to find the differences among different groups. Kaplan-Meier survival curves for overall survival were generated, and the log-rank test was used to identify the difference among different groups. The level of statistical significance was set at $P < .05$.

Results

All rabbits with VX2 tumors underwent the procedures according to the schedule for different groups. Until the 18th day of experiment, no severe complications or death were encountered. There was no significant difference in mean pretreatment animal weights ($P > .05$) and tumor volumes ($P > .05$) among these groups. RFA was performed for rabbits in group B. There was no significant difference of volumes of residual tumor between group B1 and group B2 ($P > .05$) (Table 1).

Five rabbits in each group were selected randomly and sacrificed at the 5th day, the 11th day, and the 18th day of experiment, respectively. The histopathologic evaluation was performed for the excised tumor tissue. The results of the TVGR, percentage of necrosis area, MVD, apoptosis index, and metastatic score at the fifth day of experiment were listed in Table 2.

Significant differences were found among these groups ($P < .05$), except for the metastatic score in all groups ($P = .638$) and TVGR between group B1 and group B2 ($P = .606$). At the 11th day of experiment, there was no significant difference of TVGR, percentage of necrosis area, MVD, and apoptosis index between group A and group B2 ($P > .05$). However, significant differences were found between group B1 and group A or group B2 ($P < .05$). The difference of metastatic score showed no significance among these groups ($P = .074$) (Table 3).

The findings of percentage of necrosis area, MVD, and apoptosis index at the 18th day of experiment were similar to those at the 11th day (Figure 2). There was significant difference of TVGR among these groups at the 18th day of experiment. The metastatic score of group A was significantly higher than that of group B1 ($P = .015$). But the differences of metastatic score between group A and group B2, or group B1 and group B2 were not significant (Table 4). The CEUS images at different time points were shown in Figure 3, and the changing curves of these parameters in each group were drawn (Figure 4).

The remaining five animals in each group were followed up and were humanely euthanized when they met the criteria of the end point. Two rabbits were followed up until the 90th day of experiment in group B1 and group B2, respectively. The survival curves were drawn based on the survivals of the animals (Figure 5). The median/range interquartile of survival time in groups A, B1, and B2 were 25/8 days, 50/19 days, and 48/20 days, respectively. The log-rank test revealed that significant difference was discerned between group A and group B1 ($\chi^2 = 9.701$, $P = .002$) or group B2 ($\chi^2 = 9.701$, $P = .002$). No significant difference was found between group B1 and group B2 ($\chi^2 = 0.139$, $P = .710$).

Discussion

For patients who are not suitable for surgery, RFA is considered as a first-line treatment for HCC with size less than 3 cm and no more than three lesions. However, it has been shown that local recurrence occurs more frequently after RFA treatment. Therefore, the need arises to further develop the RFA technique to increase the ablation zone so as to improve the efficacy of this treatment. The antitumor effect of RFA combined with ultrasonic cavitation was compared with RFA alone in this study, and the results showed that the necrotic area and apoptosis index were increased and the MVD was decreased in the combined group, which improved the treatment efficacy for VX2 liver tumor in rabbit model.

There are several reasons for incomplete ablation by RFA. On one hand, heat-sink effect, namely, the dissipation of the thermal output by blood flowing through adjacent vessels, could decrease the efficacy

Table 1. Comparison of Animal Weights, Tumor Volumes, and Residual Tumor Among These Three Groups

	Animal Weights (kg)	Tumor Volumes (cm^3)	Volumes of Residual Tumor (cm^3)
Group A	2.98 ± 0.21	2.59 ± 0.80	/
Group B1	2.91 ± 0.29	2.70 ± 0.76	1.94 ± 0.80
Group B2	2.96 ± 0.24	2.84 ± 0.73	2.15 ± 0.76
F/t	0.356	0.527	0.863
P	.702	.593	.393

Table 2. Compared Results at the Fifth Day of Experiment Among These Groups

	TVGR (%)	Percentage of Necrosis Area (%)	MVD (/Field)	Apoptosis Index (/Field)	Metastatic Score
Group A	22.54 ± 15.40*	20.48 ± 5.29	52.08 ± 4.69	1.60 ± 0.62	0/1.5
Group B1	−4.21 ± 4.37	60.28 ± 7.46*	23.36 ± 1.73*	5.16 ± 0.59*	0/0.5
Group B2	−1.06 ± 2.90	45.44 ± 10.07*	34.80 ± 3.96*	3.28 ± 0.75*	0/0.5
F/H	12.119	32.777	76.970	36.738	0.900
P	.001	.000	.000	.000	.638

* The significant difference could be found between this group and both the other two groups by pairwise comparison.

Table 3. Compared Results at the 11th Day of Experiment Among These Groups

	TVGR (%)	Percentage of Necrosis Area (%)	MVD (/Field)	Apoptosis Index (/Field)	Metastatic Score
Group A	58.14 ± 40.41	32.70 ± 3.24	47.28 ± 5.67	1.80 ± 0.86	2/0.5
Group B1	−6.59 ± 3.51*	55.62 ± 4.78*	24.16 ± 2.22*	4.24 ± 0.34*	0/1.5
Group B2	26.95 ± 10.80	38.20 ± 4.79	45.12 ± 5.47	2.36 ± 0.76	1/1.5
F/H	8.919	38.181	36.516	17.124	5.195
P	.004	.000	.000	.000	.074

* The significant difference could be found between this group and both the other two groups by pairwise comparison.

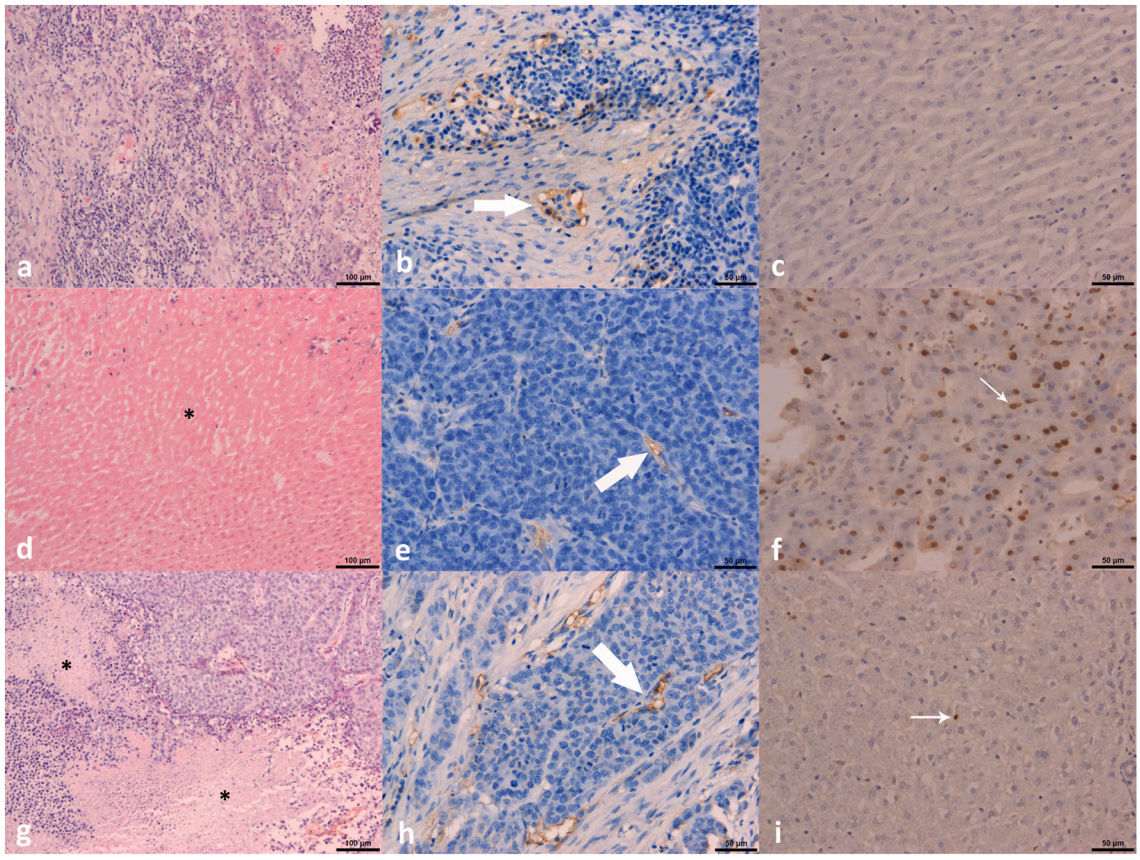

Figure 2. The findings of H&E staining (×100; figures A, D, G), MVD (×200; figures B, E, H) and apoptosis (×200; figures C, F, I) at the 18th day of experiment. Figures A-C were group A, D-F were group B1, and G-I were group B2. The asterisk in figure D and G showed the necrosis area. Large arrows in figure B, E, and H demonstrated the microvessel. Small arrows in figure F and I indicated the positive staining of apoptosis cells.

of the procedure and induce local tumor recurrences [37], which is associated with the distance between lesion and vessel as well as the flow velocity in the vessel. Lin et al. showed that the recurrence rate of perivascular lesions was higher than that of nonperivascular lesions [38]. On the other hand, the location of tumor near to crucial organs, such as gallbladder or gastrointestinal tract, or larger lesion relative to ablative zone, induces inability to achieve the safety margin and results in local recurrence [39].

To overcome this problem, various combined therapies have been investigated in previous studies. There is increasing evidence that combining RFA to TACE may increase the therapeutic benefit in large HCCs. A meta-analysis of eight randomized controlled trials including 598 patients indicated that RFA plus TACE determines a significantly higher 3-year overall survival rate (odds ratio: 2.65, 95% confidence interval: 1.81-3.86, $P < .001$) and 3-year recurrence free survival rate (odds ratio: 3.00, 95% confidence interval: 1.75-5.13, $P < .001$) than RFA alone, with no difference in major complications (odds ratio: 1.20, 95% confidence interval: 0.31-4.62, $P = .79$) [40]. Additionally, comparative studies have also been performed between RFA alone and in combination with percutaneous ethanol injection (PEI). Shankar et al. [41] have reported achieving a significantly larger ablation volume with combined therapy (84.6 cm^2) than with RFA alone (32.3 cm^2) with no increase in the complication rate. The findings of a study from Zhang et al. [39] showed that overall survival rates with RFA alone were significantly less than RFA combined with PEI. However, in their study, the size of enrolled lesions was between 3.0 cm and 5.0 cm. In routine clinical practices, a large proportion of enrolled patients for RFA have lesions less than 3.0 cm in diameter. Kalra et al. [42] reported that there was no significant difference that could be found in the survival time as well as the local recurrences and the distant intrahepatic recurrences in RFA alone compared to RFA combined with PEI, in which majority of the tumor was less than 3.0 cm. Hence, it is necessary to explore a novel combined treatment for RFA to increase the antitumor effect for liver tumors.

Table 4. Compared Results at the 18th Day of Experiment Among These Groups

	TVGR (%)	Percentage of Necrosis Area (%)	MVD (/field)	Apoptosis Index (/Field)	Metastatic Score
Group A	121.11 ± 33.79	40.58 ± 3.92	46.08 ± 3.24	1.42 ± 0.38	3/1
Group B1	3.70 ± 9.48 *	55.50 ± 5.23 *	25.28 ± 3.08 *	2.80 ± 0.42 *	1/1.5
Group B2	54.37 ± 18.22 *	40.26 ± 2.26	47.52 ± 3.66	1.66 ± 0.44	2/1
F/H	33.260	23.805	69.611	15.833	8.076
P	.000	.000	.000	.000	.018

* The significant difference could be found between this group and both the other two groups by pairwise comparison.

As a process required for invasion and metastasis, tumor angiogenesis constitutes an important point of control of cancer progression [43]. Generally, antiangiogenic therapy that targets multiple angiogenic pathways has been considered as a potential effective method for treatment of advanced solid tumors. In addition to antiangiogenic agents, physical therapy could also be used to inhibit tumor angiogenesis. Ultrasonic cavitation can result in

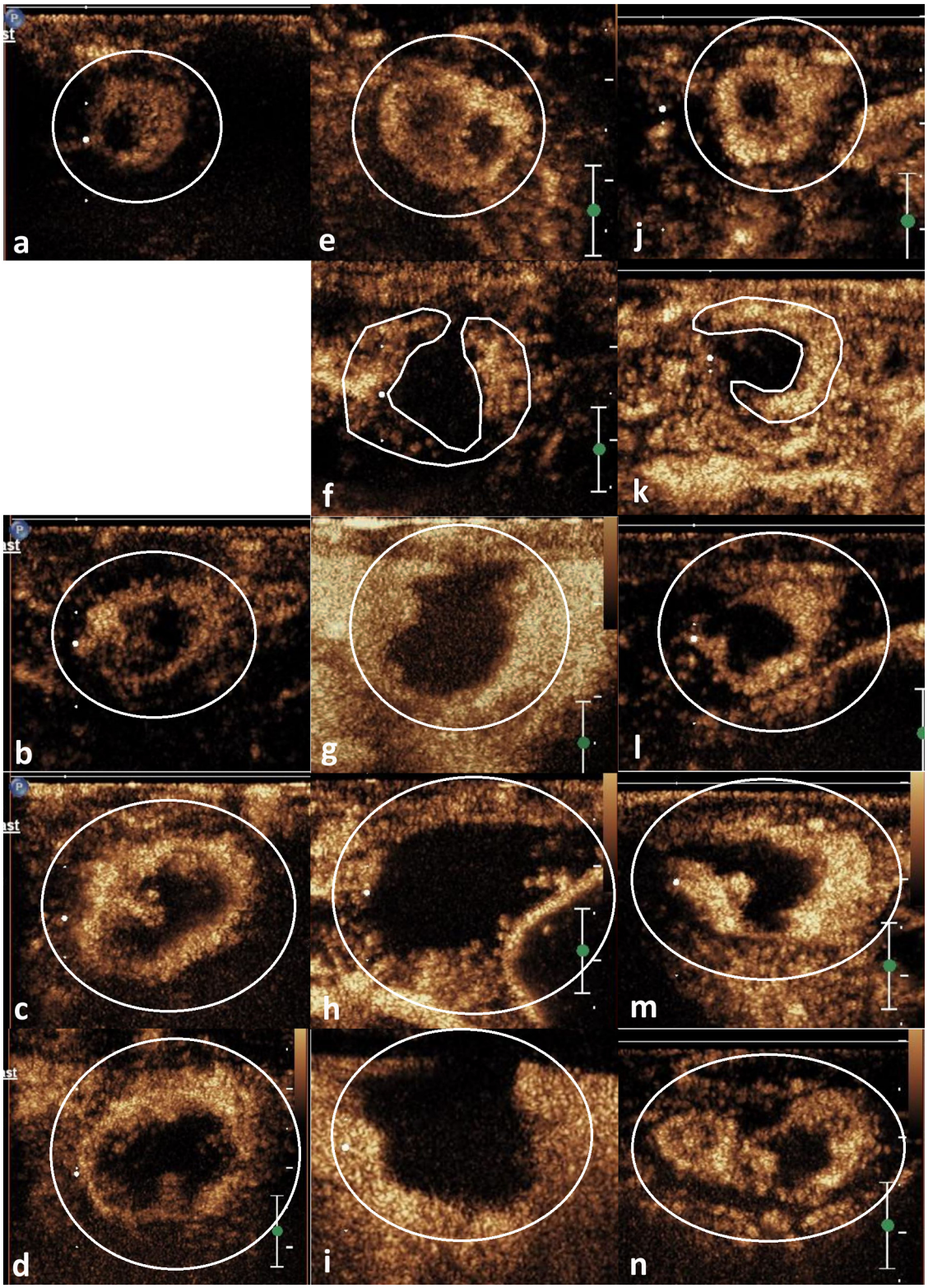

Figure 3. CEUS images at different time points (before RFA: A, E, J; immediately after RFA: F, K; the 5th day: B, G, L; the 11th day: C, H, M; the 18th day: D, I, N) for these three groups. Figures A-D were group A, E-I were group B1, and J-N were group B2. The viable tumor tissue appeared as hyperenhancement by CEUS (shown by the marker lines). The tumor size was gradually increasing in groups A and B2.

hemorrhage, edema, thrombus formation, and damage to the endothelium of capillaries or small vessels, which can induce necrosis and apoptosis of cancer cells and inhibit tumor growth. In the study from Wang et al., the antitumor effect of microbubbles enhanced by low-frequency ultrasound cavitation on prostate carcinoma was investigated, and the results showed that the gross tumor volume, microvessel density, and the average optical density of vascular endothelial growth factor could be decreased by ultrasound irradiation plus microbubbles [22]. Huang et al. reported that ultrasound mediated microbubbles destruction could be used as a

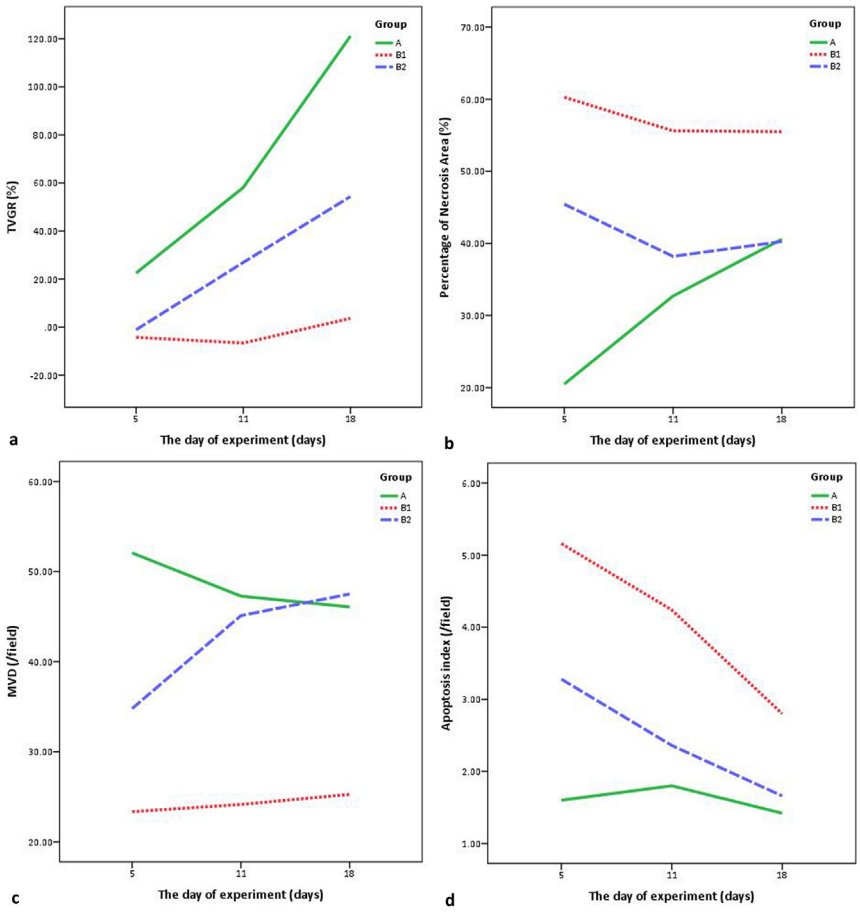

Figure 4. The changing curves of TVGR (A), percentage of necrosis area (B), MVD (C), and apoptosis index (D).

promising novel therapeutic strategy to treat colon cancer, which could inhibit the tumor growth, the expression of CD31, and metastasis [25].

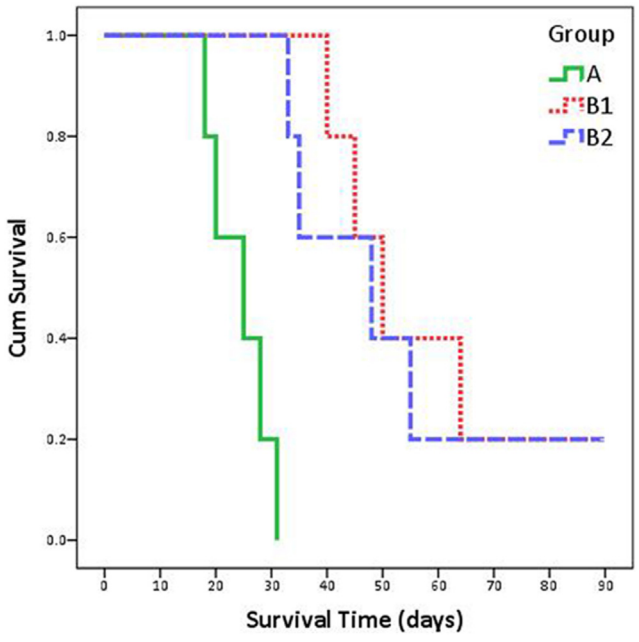

Figure 5. The survival curves of these three groups.

In this study, ultrasonic cavitation was performed for VX2 liver tumors in rabbit model following incomplete RFA, and the antitumor effect was compared with control group as well as RFA alone group. The results showed that not only the tumor volume but also the histopathological findings in RFA plus ultrasonic cavitation group were improved by compared to RFA alone and control groups significantly. Ultrasonic cavitation could present the effect of antiangiogenesis and cause a series of pathological changes such as absence of nucleus membrane, chromatin condensation, mitochondrial vacuolation, and hemorrhagic damage of microvessel [44,45], which increase the necrotic area and apoptosis, decrease the microvessle density, and then inhibit the tumor volume enlargement. The circulating microbubbles take effect as cavitation nucleus to enhance the inertial cavitation. During the therapy, 9-second pause followed by 1-second irradiation was helpful for perfusion of abundant microbubbles into residual tumor tissue and for avoiding heat accumulation in the irradiation zone. There were 9 irradiation points for each lesion, 15 therapy cycles for each point, and 3 consecutive days of cavitation treatment, which enhanced the therapeutic effect further.

However, the metastasis score and survival time were not significantly ameliorated by ultrasonic cavitation after RFA. The possible reasons about these findings may be the relatively small number of cases (five cases in each group in each point-in-time) and the sequence of RFA and cavitation might be not optimal. According to the experiences of TACE combined with RFA from published literature [46–49], TACE performed before RFA could be helpful to

block the tumor vessels and decrease the heat-sink effect of RFA. Therefore, optimal therapeutic schedules of combination of RFA and ultrasonic cavitation should be further investigated.

There were some limitations to this study. First, the temperature in the sonicated tumor tissue, which may be elevated in some degrees, had not been monitored during cavitation in this study. Second, different tumor location and fat content of rabbit liver may present different acoustic attenuation, which may influence the acoustic intensity for treatment weakly. Third, the difference of residual tumor volume between group B1 and group B2 was evaluated by imaging modality (CEUS), which may be affected by the zone of hyperemia and edema surrounding the ablation area after RFA.

Conclusion

Ultrasonic cavitation after incomplete RFA for VX2 liver tumor improved the antitumor effect, which could be considered as a potentially therapeutic strategy for liver malignancy.

Acknowledgements

The authors would like to acknowledge the colleagues from department of pathology and general surgery of Sir Run Run Shaw Hospital, Zhejiang University, School of Medicine, for their help of this study. This research was supported by the National Natural Science Foundation of China (grant nos. 81402569, 81527803, 81420108018), National Key R&D Program of Chinaof China (no. 2018YFC0115900), and Zhejiang Science and Technology Project (no. 2019C03077), which are gratefully acknowledged and with none declared conflict of interest

References

[1] Bray F, Ferlay J, Soerjomataram I, Siegel RL, Torre LA, and Jemal A (2018). Global cancer statistics 2018: GLOBOCAN estimates of incidence and mortality worldwide for 36 cancers in 185 countries. *CA Cancer J Clin* **68**, 394–424. http://dx.doi.org/10.3322/caac.21492.

[2] Torre LA, Bray F, Siegel RL, Ferlay J, Lortet-Tieulent J, and Jemal A (2015). Global cancer statistics, 2012. *CA Cancer J Clin* **65**, 87–108. http://dx.doi.org/10.3322/caac.21262.

[3] Llovet JM, Burroughs A, and Bruix J (2003). Hepatocellular carcinoma. *Lancet* **362**, 1907–1917. http://dx.doi.org/10.1016/S0140-6736(03)14964-1.

[4] Song TJ, Ip EW and Fong Y (2004). Hepatocellular carcinoma: current surgical management. Gastroenterology 127, S248-S260. PMID: 15508091

[5] Lau WY and Lai EC (2009). The current role of radiofrequency ablation in the management of hepatocellular carcinoma: a systematic review. *Ann Surg* **249**, 20–25. http://dx.doi.org/10.1097/SLA.0b013e31818eec29.

[6] El-Serag HB (2011). Hepatocellular carcinoma. *N Engl J Med* **365**, 1118–1127. http://dx.doi.org/10.1056/NEJMra1001683.

[7] Yang JD and Roberts LR (2010). Epidemiology and management of hepatocellular carcinoma. *Infect Dis Clin North Am* **24**, 899–919, viii. http://dx.doi.org/10.1016/j.idc.2010.07.004.

[8] Shiina S, Tateishi R, Arano T, Uchino K, Enooku K, Nakagawa H, Asaoka Y, Sato T, Masuzaki R, and Kondo Y, et al (2012). Radiofrequency ablation for hepatocellular carcinoma: 10-year outcome and prognostic factors. *Am J Gastroenterol* **107**, 569–577 quiz 578 https://doi.org/10.1038/ajg.2011.425.

[9] Curley SA, Izzo F, Ellis LM, Nicolas Vauthey J, and Vallone P (2000). Radiofrequency ablation of hepatocellular cancer in 110 patients with cirrhosis. *Ann Surg* **232**, 381–391 [PMID: 10973388].

[10] Komorizono Y, Oketani M, Sako K, Yamasaki N, Shibatou T, Maeda M, Kohara K, Shigenobu S, Ishibashi K, and Arima T (2003). Risk factors for local recurrence of small hepatocellular carcinoma tumors after a single session, single application of percutaneous radiofrequency ablation. *Cancer* **97**, 1253–1262. http://dx.doi.org/10.1002/cncr.11168.

[11] Ruzzenente A, Manzoni GD, Molfetta M, Pachera S, Genco B, Donataccio M and Guglielmi A (2004). Rapid progression of hepatocellular carcinoma after Radiofrequency Ablation. World J Gastroenterol 10, 1137–1140. PMID: 15069713

[12] Tajima H, Ohta T, Okamoto K, Nakanuma S, Hayashi H, Nakagawara H, Onishi I, Takamura H, Kitagawa H, and Fushida S, et al (2010). Radiofrequency ablation induces dedifferentiation of hepatocellular carcinoma. *Oncol Lett* **1**, 91–94. http://dx.doi.org/10.3892/ol_00000016.

[13] Zhang N, Wang L, Chai ZT, Zhu ZM, Zhu XD, Ma DN, Zhang QB, Zhao YM, Wang M, and Ao JY, et al (2014). Incomplete radiofrequency ablation enhances invasiveness and metastasis of residual cancer of hepatocellular carcinoma cell HCCLM3 via activating β-catenin signaling. *PLoS One* **9**e115949. http://dx.doi.org/10.1371/journal.pone.0115949.

[14] Zolochevska O and Figueiredo ML (2012). Advances in sonoporation strategies for cancer. Front Biosci (Schol Ed) 4, 988–1006. PMID: 22202104

[15] Marmottant P and Hilgenfeldt S (2003). Controlled vesicle deformation and lysis by single oscillating bubbles. *Nature* **423**, 153–156. http://dx.doi.org/10.1038/nature01613.

[16] Miller MW, Miller DL and Brayman AA (1996). A review of in vitro bioeffects of inertial cavitation from a mechanistic perspective. Ultrasound Med Biol 22, 1131–1154. PMID: 9123638

[17] Chen H, Brayman AA, Bailey MR, and Matula TJ (2010). Blood vessel rupture by cavitation. *Urol Res* **38**, 321–326. http://dx.doi.org/10.1007/s00240-010-0302-5.

[18] Li P, Armstrong WF, Miller DL, Bluemke DA, Sheth S, Magee CA, Horton KM, Eng J, and Fishman EK (2004). Impact of myocardial contrast echocardiography on vascular permeability: Comparison of three different contrast agents. *Ultrasound Med Biol* **30**, 83–91. http://dx.doi.org/10.1016/j.ultrasmedbio.2003.09.004.

[19] Sheikov N, McDannold N, Vykhodtseva N, Jolesz F, and Hynynen K (2004). Cellular mechanisms of the blood-brain barrier opening induced by ultrasound in presence of microbubbles. *Ultrasound Med Biol* **30**, 979–989. http://dx.doi.org/10.1016/j.ultrasmedbio.2004.04.010.

[20] Burke CW and Price RJ (2010). Contrast ultrasound targeted treatment of gliomas in mice via drug-bearing nanoparticle delivery and microvascular ablation. *J Vis Exp* . http://dx.doi.org/10.3791/2145 pii, 2145.

[21] Wood AK and Sehgal CM (2015). A review of low-intensity ultrasound for cancer therapy. *Ultrasound Med Biol* **41**, 905–928. http://dx.doi.org/10.1016/j.ultrasmedbio.2014.11.019.

[22] Wang Y, Hu B, Diao X, and Zhang J (2012). Antitumor effect of microbubbles enhanced by low frequency ultrasound cavitation on prostate carcinoma xenografts in nude mice. *Exp Ther Med* **3**, 187–191. http://dx.doi.org/10.3892/etm.2011.377.

[23] Hu X, Kheirolomoom A, Mahakian LM, Beegle JR, Kruse DE, Lam KS, and Ferrara KW (2012). Insonation of targeted microbubbles produces regions of reduced blood flow within tumor vasculature. *Invest Radiol* **47**, 398–405. http://dx.doi.org/10.1097/RLI.0b013e31824bd237.

[24] Zhong Y, Liu Z, Zhu M, Gao SJ, Gao WH, Qiao L, Wu SZ, Liu Q, and Tan KB (2012). Destruction of Walker-256 tumor vasculature by a novel ultrasound cavitation technique. *Zhonghua Yi Xue Za Zhi* **92**, 487–490. http://dx.doi.org/10.3760/cma.j.issn.00376-2491-2012.07.015.

[25] Huang P, You X, Pan M, Li S, Zhang Y, Zhao Y, Wang M, Hong Y, Pu Z, and Chen L, et al (2013). A novel therapeutic strategy using ultrasound mediated microbubbles destruction to treat colon cancer in a mouse model. *Cancer Lett* **335**, 183–190. http://dx.doi.org/10.1016/j.canlet.2013.02.011.

[26] Zhang C, Huang P, Zhang Y, Chen J, Shentu W, Sun Y, Yang Z, and Chen S (2014). Anti-tumor efficacy of ultrasonic cavitation is potentiated by concurrent delivery of anti-angiogenic drug in colon cancer. *Cancer Lett* **347**, 105–113. http://dx.doi.org/10.1016/j.canlet.2014.01.022.

[27] Forner A, Reig M, and Bruix J (2018). Hepatocellular carcinoma. *Lancet* **391**, 1301–1314. http://dx.doi.org/10.1016/S0140-6736(18)30010-2.

[28] Bholee AK, Peng K, Zhou Z, Chen J, Xu L, Zhang Y, and Chen M (2017). Radiofrequency ablation combined with transarterial chemoembolization versus hepatectomy for patients with hepatocellular carcinoma within Milan criteria: a retrospective case-control study. *Clin Transl Oncol* **19**, 844–852. http://dx.doi.org/10.1007/s12094-016-1611-0.

[29] Tang Z, Kang M, Zhang B, Chen J, Fang H, Ye Q, Jiang B, and Wu Y (2017). Advantage of sorafenib combined with radiofrequency ablation for treatment of hepatocellular carcinoma. *Tumori* **103**, 286–291. http://dx.doi.org/10.5301/tj.5000585.

[30] Zhao LY, Liu S, Chen ZG, Zou JZ, and Wu F (2017). Cavitation enhances coagulated size during pulsed high-intensity focussed ultrasound ablation in an isolated liver perfusion system. *Int J Hyperthermia* **33**, 343–353. http://dx.doi.org/10.1080/02656736.2016.1255918.

[31] Daecher A, Stanczak M, Liu JB, Zhang J, Du S, Forsberg F, Leeper DB, and Eisenbrey JR (2017). Localized microbubble cavitation-based antivascular therapy for improving HCC treatment response to radiotherapy. *Cancer Lett* **411**, 100–105. http://dx.doi.org/10.1016/j.canlet.2017.09.037.

[32] Haaga JR, Exner AA, Wang Y, Stowe NT, and Tarcha PJ (2005). Combined tumor therapy by using radiofrequency ablation and 5-FU-laden polymer implants: evaluation in rats and rabbits. *Radiology* **237**, 911–918. http://dx.doi.org/10.1148/radiol.2373041950.

[33] Schneider M, Arditi M, Barrau MB, Brochot J, Broillet A, Ventrone R and Yan F (1995). BR1: a new ultrasonographic contrast agent based on sulfur hexafluoride-filled microbubbles. Invest Radiol 30, 451–457. PMID: 8557510

[34] Rapoport N, Pitt WG, Sun H and Nelson JL (2003). Drug delivery in polymeric micelles: from in vitro to in vivo. J Control Release 91, 85–95. PMID: 12932640

[35] Weidner N (1995). Current pathologic methods for measuring intratumoral microvessel density within breast carcinoma and other solid tumors. Breast Cancer Res Treat 36, 169–180. PMID: 8534865

[36] Duan WR, Garner DS, Williams SD, Funckes-Shippy CL, Spath LS, and Blomme EA (2003). Comparison of immunohistochemistry for activated caspase-3 and cleaved cytokeratin 18 with the TUNEL method for quantification of apoptosis in histological sections of PC-3 subcutaneous xenografts. *J Pathol* **199**, 221–228. http://dx.doi.org/10.1002/path.1289.

[37] Jacobs A (2015). Radiofrequency ablation for liver cancer. *Radiol Technol* **86**, 645–664 quiz 665-668. PMID: 26199436.

[38] Lin ZY, Li GL, Chen J, Chen ZW, Chen YP, and Lin SZ (2016). Effect of heat sink on the recurrence of small malignant hepatic tumors after radiofrequency ablation. *J Cancer Res Ther* **12**, C153–C158. http://dx.doi.org/10.4103/jcrt.JCRT_959_16.

[39] Zhang YJ, Liang HH, Chen MS, Guo RP, Li JQ, Zheng Y, Zhang YQ, and Lau WY (2007). Hepatocellular carcinoma treated with radiofrequency ablation with or without ethanol injection: A prospective randomized trial. *Radiology* **244**, 599–607. http://dx.doi.org/10.1148/radiol.2442060826.

[40] Ni JY, Liu SS, Xu LF, Sun HL, and Chen YT (2013). Meta-analysis of radiofrequency ablation in combination with transarterial chemoembolization for hepatocellular carcinoma. *World J Gastroenterol* **19**, 3872–3882. http://dx.doi.org/10.3748/wjg.v19.i24.3872.

[41] Shankar S, vanSonnenberg E, Morrison PR, Tuncali K, and Silverman SG (2004). Combined radiofrequency and alcohol injection for percutaneous hepatic tumor ablation. *AJR Am J Roentgenol* **183**, 1425–1429. http://dx.doi.org/10.2214/ajr.183.5.1831425.

[42] Kalra N, Kang M, Duseja AK, Bhatia A, Singh V, Dhiman RK, Rajwanshi A, Chawla YK, and Khandelwal N (2017). Comparison of radiofrequency ablation alone & in combination with percutaneous ethanol injection for management of hepatocellular carcinoma. *Indian J Med Res* **146**, S30–S37. http://dx.doi.org/10.4103/ijmr.IJMR_1812_15.

[43] Zhao Y and Adjei AA (2015). Targeting angiogenesis in cancer therapy: moving beyond vascular endothelial growth factor. *Oncologist* **20**, 660–673. http://dx.doi.org/10.1634/theoncologist.2014-0465.

[44] Luo W, Wen G, Yang L, Tang J, Wang J, Wang J, Zhang S, Zhang L, Ma F, and Xiao L, et al (2017). Dual-targeted and pH-sensitive doxorubicin prodrug-microbubble complex with ultrasound for tumor treatment. *Theranostics* **7**, 452–465. http://dx.doi.org/10.7150/thno.16677.

[45] Hua X, Ding J, Li R, Zhang Y, Huang Z, Guo Y, and Chen Q (2016). Anti-tumor effect of ultrasound-induced Nordy-loaded microbubbles destruction. *J Drug Target* **24**, 703–708. http://dx.doi.org/10.3109/1061186X.2016.1144058.

[46] Peng ZW, Zhang YJ, Liang HH, Lin XJ, Guo RP, and Chen MS (2012). Recurrent hepatocellular carcinoma treated with sequential transcatheter arterial chemoembolization and RF ablation versus RF ablation alone: a prospective randomized trial. *Radiology* **262**, 689–700. http://dx.doi.org/10.1148/radiol.11110637.

[47] Yang W, Chen MH, Wang MQ, Cui M, Gao W, Wu W, Wu JY, Dai Y, and Yan K (2009). Combination therapy of radiofrequency ablation and transarterial chemoembolization in recurrent hepatocellular carcinoma after hepatectomy compared with single treatment. *Hepatol Res* **39**, 231–240. http://dx.doi.org/10.1111/j.1872-034X.2008.00451.x.

[48] Shibata T, Isoda H, Hirokawa Y, Arizono S, Shimada K, and Togashi K (2009). Small hepatocellular carcinoma: is radiofrequency ablation combined with transcatheter arterial chemoembolization more effective than radiofrequency ablation alone for treatment? *Radiology* **252**, 905–913. http://dx.doi.org/10.1148/radiol.2523081676.

[49] Morimoto M, Numata K, Kondou M, Nozaki A, Morita S, and Tanaka K (2010). Midterm outcomes in patients with intermediate-sized hepatocellular carcinoma: a randomized controlled trial for determining the efficacy of radiofrequency ablation combined with transcatheter arterial chemoembolization. *Cancer* **116**, 5452–5460. http://dx.doi.org/10.1002/cncr.25314.